Generation of flat-spectrum wideband chaos by fiber ring resonator

Anbang Wang (王安帮), Yuncai Wang (王云才),[a] Yibiao Yang (杨毅彪), Mingjiang Zhang (张明江), Hang Xu (徐航), and Bingjie Wang (王冰洁)
Key Laboratory of Advanced Transducers & Intelligent Control System, Ministry of Education, Taiyuan University of Technology, Taiyuan 030024, China and Institute of Optoelectronic Engineering, College of Physics & Optoelectronics, Taiyuan University of Technology, Taiyuan 030024, China

(Received 8 November 2012; accepted 8 January 2013; published online 24 January 2013)

We present a simple method to generate spectrally uniform wideband chaos by injecting chaotic laser into a fiber ring resonator. The resonator is a single-coupler ring equipped with an optical filter and amplifier, which adjust the optical field circulating in the ring. The incoherent interference of the circulating fields produces wideband chaos with uniform power spectrum density distribution. We experimentally achieved a chaotic spectrum that extends over 26.5 GHz (limited by measurement bandwidth) and fluctuates within ±1.5 dB. In addition, tuning the filter frequency can control the spectral profile so as to meet different application needs. © *2013 American Institute of Physics*. [http://dx.doi.org/10.1063/1.4789366]

Optical chaos has attracted widespread attention in recent years because of its important applications, for instance, in encrypted communications,[1,2] physical random number generation,[3,4] lidar,[5] and time domain reflectometry.[6,7] The key to these applications is a compact and broadband chaotic light source. And a semiconductor laser with optical feedback[1–4,6–8] is usually the common choice owing to its simple and integratable setup. Although recent years have found some reports on several photonic integrated sources based on optical feedback laser diode,[9–11] the bandwidth is normally limited below 10 GHz, because relaxation oscillation of laser dominates the power spectral density (PSD) of chaotic light.[12] Consequently, both the message transmission rates in chaos-based communications[1] and the generation rate of random number using chaotic semiconductor laser[13] are greatly restricted.

Many efforts have been devoted to the increase of the bandwidth of chaotic laser. Some studies found that optical injection from a chaotic laser into a static laser or conversely can expand the bandwidth of chaotic signal up to 20 GHz.[14–18] And still others show that dual injection from two external lasers can further enlarge it.[19,20] However, the schemes of the injection methods are complex and delicate, because two or three lasers should be matched in terms of multi parameters. Moreover, the dominant laser relaxation oscillation leads to a nonuniform power density distribution.[14–20] Resultantly, the low energy in low-frequency band (below the relaxation oscillation frequency) reduces the utilization efficiency of chaotic light because most electronic acquisition devices act like a low-pass filter. Although electro-optic or optoelectronic oscillators can generate flatter chaotic spectrum than optical injection method,[21–23] high-speed modulators and wideband electronic amplifiers are costly.

Fiber ring resonators (FRRs) are widely used as interferometers, filters, modulators, wavelength-selective switches,[24–27] and so on. Here, we experimentally demonstrate and theoretically simulate that the all-optical fiber ring resonator, acting as a bandwidth enhancer, can directly widen a narrowband chaotic signal over 26.5 GHz. Furthermore, it can also reshape the spectral profile, that is, remove the peak feature of relaxation frequency and flatten the whole spectrum. In addition, it can control the spectral width naturally without loss in energy.

As shown in Fig. 1, the experimental setup consists of an optical-feedback semiconductor laser used to emit a narrowband chaotic light and a fiber ring resonator serving as bandwidth enhancer. The FRR is equipped with an optical filter and an amplifier. The filter is a tunable fiber Bragg grating with linewidth of about 20 GHz, which is inserted in the ring through a circulator, and the amplifier is an erbium-doped fiber amplifier (EDFA, ACCELINK EDFA-BA-1550) with an inbuilt isolator which avoids stimulated Brillouin backscattering light. The round-trip time of the ring was 192.4 ns, and the intra-ring loss was about −4.9 dB. The chaotic laser was a distributed feedback (DFB) laser diode (WTD LDM5S752) with optical feedback from an external mirror. The DFB laser was stabilized at 1554.23 nm by a precise temperature controller, and was biased with a current of 1.68 times threshold, which yields 4 GHz of relaxation frequency. We used a 47 GHz photodetector (u^2t XPDV2120R) followed by a RF spectrum analyzer (Agilent N9020A) with cutoff frequency of 26.5 GHz to measure the spectrum of

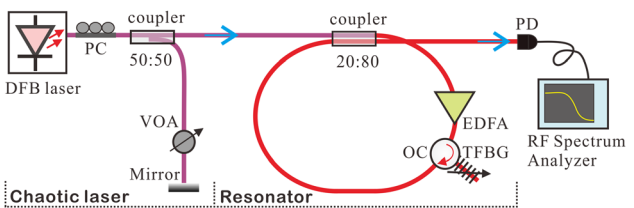

FIG. 1. Experimental setup. The resonator consists of a fiber ring equipped with an EDFA and a tunable fiber Bragg grating (TFBG). A DFB laser diode with external-cavity feedback from a mirror is used as the chaotic injection source. The spectral property of chaotic signal is measured by a RF spectrum analyzer. PC: polarization controller; VOA: variable optical attenuator; OC: optical circulator; PD: photodetector.

[a]Author to whom correspondence should be addressed. Electronic mail: wangyc@tyut.edu.cn.

chaotic light. For assistance, a real time oscilloscope with 4 GHz bandwidth (Agilent MSO9404A) and an optical spectrum analyzer with 0.06 nm resolution (Agilent 86140B) were employed to record time series and optical spectrum, respectively.

Under the feedback strength of −14.5 dB and delay of 94.2 ns, the optical-feedback laser diode generated a chaotic light with power of −0.79 dBm. The power spectral density of the chaotic laser light is shown in Fig. 2 with black curve (blue online). It can be found that an obvious peak appears at the relaxation frequency, which is about 18 dB higher than the lowest component. The sharp band-pass spectral profile caused by the energy concentration in a narrow band limits the effective bandwidth and signal energy utilization.

By injecting the chaotic light into the resonator and tuning the filter frequency ν_F as 25 GHz relative to the laser frequency ν_0, we found the power spectrum (gray or cyan curve in Fig. 2) expands flatly up to the cutoff frequency of the RF spectrum analyzer. Note that after subtraction of the noise background of the analyzer, the output spectrum (dark gray or red) is still flat. To be specific, it fluctuates within a range of only ±1.5 dB with a standard deviation of 0.97 dB. Compared with the previous results,[14,17,19] ours are much flatter: not only are the high-frequency oscillations excited but also the low-frequency components are enhanced greatly; furthermore, the peak of relaxation oscillation is eliminated. The increase in amplitude of time series (see the left inset), recorded by the 4 GHz oscilloscope, definitely shows the low frequency energy enhancement. Note that the largest Lyapunov exponent of the time series is also increased from 1.34 ns^{-1} up to about 2.43 ns^{-1} calculated with the method proposed by Rosenstein *et al.*[28]

Apart from spectrum improvement, the resonator also enlarges the power of chaotic light. Circulating in the ring, the light gains round and round until the amplifier turns saturated. After a short time, the output power of the resonator equals to the difference between the amplifier saturation power and the ring loss. In our experiment, the amplifier's saturation power was 12.2 dBm at 120 mA pump current, the total loss was −5.9 dB, and thus, the light power raised from −0.79 to 6.3 dBm. As shown by the right inset in Fig. 2, the gain was mainly supplied to the mode selected by the filter which broadened the optical spectrum.

We experimentally studied the effects of the gain on the spectrum by adjusting the pump current of the EDFA. Fixing the filter detuning at 25 GHz results in several output light at different gain levels. Figure 3(a) shows their power spectral density and Fig. 3(b) plots the corresponding optical spectra. As shown by the curve (1), a small gain raises the low-frequency part to the extent that the spectrum turns into a flat low-pass profile. When the gain at the filter mode grows to a critical value of about 25.8 dB, high-frequency oscillations beyond 15 GHz are excited over the noise floor, shown by curve (2) in Fig. 3(a). The corresponding optical spectrum in Fig. 3(b) reveals that this critical gain makes the power of the filtered frequency equivalent to the central mode at 0 GHz. The gain larger than the critical value can significantly expand the spectrum (see curves (3) and (4) in Fig. 3(a)). We define the bandwidth as width of the band from zero to the frequency which contains 80% of signal energy, and the flatness as the range of spectral fluctuation in the band. Figure 3(c) shows the detailed tendencies of bandwidth and flatness by diamonds and circles, respectively. Obviously, the resonator can improve the spectral profile and flatness (below ±3 dB) independent of gain, while the great increase of bandwidth needs a larger gain level.

We also experimentally explored the influences of filter frequency with fixed pump current 120 mA of the amplifier. Figure 4(a) displays four power spectra produced at detuning of −23.6, −17.4, 0, and 23.1 GHz, and Fig. 4(b) plots the corresponding optical spectra. Figure 4(c) shows the tendencies of bandwidth and flatness by diamonds and circles as functions of filter detuning. These results suggest that the filter should be tuned into the wings of the chaotic laser field to reach chaos beyond 15 GHz with spectral flatness below ±3 dB. As detuning decreases to zero, the bandwidth drops but spectral flatness remains almost unchanged. For example, the spectrum at zero detuning shown by curve (3) in Fig. 4 (a) still has a flat low-pass profile. Furthermore, it becomes

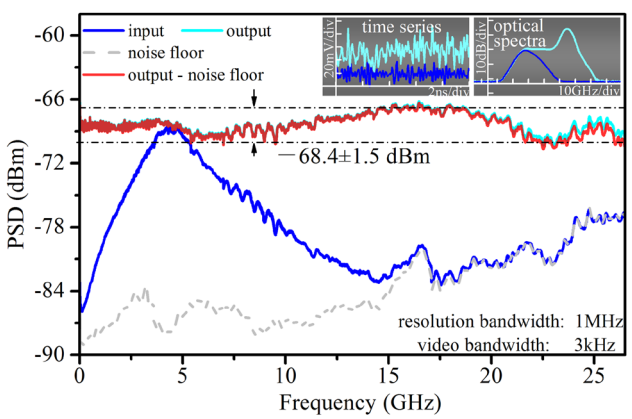

FIG. 2. Experimental improvement of PSD: the black (blue) and the gray (cyan) curves represent the chaotic laser and the fiber ring resonator output, respectively. The dark gray (red) curve is the output spectrum after subtraction of electronic noise (dashed line) of the RF spectrum analyzer. The insets plot the corresponding time series and optical spectra.

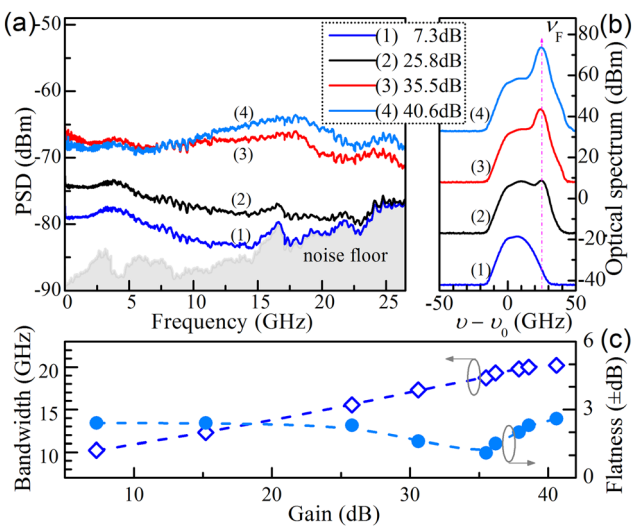

FIG. 3. Experimentally obtained effects of gain: (a) the power spectral density of the resonator outputs generated with different gains of 7.3, 25.8, 35.5, and 40.6 dB at detuning of 25 GHz, (b) the corresponding optical spectra, and (c) the bandwidth (◇) and spectral flatness (●) as the functions of gain.

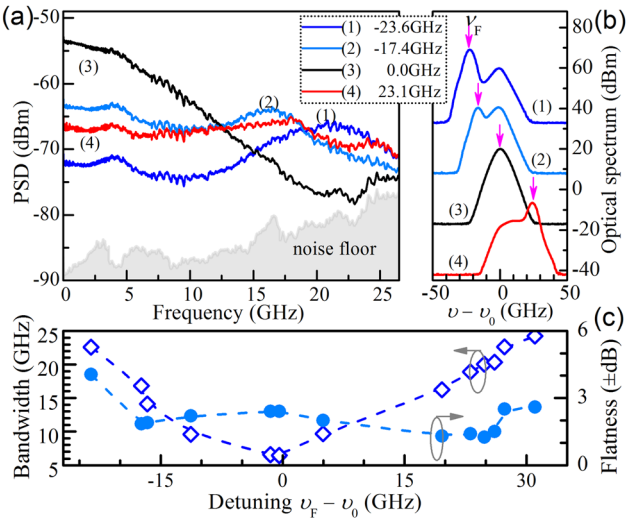

FIG. 4. Experimentally obtained effects of filter detuning: (a) the power spectral density of the resonator outputs generated at different detuning of −23.6, −17.4, 0, and 23.1 GHz with intra-ring loss of −4.9 dB, (b) the corresponding optical spectra, and (c) the bandwidth (◇) and spectral flatness (●) as the functions of filter detuning.

higher than the spectrum obtained at large detuning, which means that energy transfers from high to low frequency. Therefore, the resonator can control the spectral profile without energy consumption. We should mention that our method can achieve similar results for an undeveloped chaotic input whose spectrum has strong harmonic peaks of relaxation frequency (see Fig. S1 in supplementary material[29]).

As the experiments describe, the generation of wideband chaotic oscillation with flat band structure includes two parts, one is chaos produced by a semiconductor laser with optical feedback and the other is chaos through the ring resonator. The chaos generation in semiconductor laser with optical feedback has been well studied, and its physical mechanism can be understood as following. The external feedback destroys the balance between carrier density and photon density and thus excites relaxation oscillation, and the nonlinear frequency mixing between the excited relaxation oscillation and the external-cavity modes causes the chaotic behavior.[30] The mechanism interprets the reason why the laser relaxation oscillation dominates the chaos of laser intensity.

To get insight into the cause of the expansion of the spectrum through the FRR, we have carried out numerical simulation with single-mode Lang-Kobayashi rate equations,[31] which are typical model for optical-feedback semiconductor laser. The equations of electrical field complex amplitude $A = |A|\exp[i\varphi(t)]$ and carrier density N are written as follows:

$$\dot{A} = \frac{1}{2}(1+i\alpha)[G-\tau_p^{-1}]A + k_f A(t-\tau_f)\exp(-2\pi\nu_0\tau_f), \quad (1)$$

$$\dot{N} = J - \tau_N^{-1}N - G|A|^2, \quad (2)$$

where $G = g_d(N - N_0)/(1 + \varepsilon A^2)$, N_0 is transparency carrier density, g_d is differential gain, ε is gain saturation parameter, τ_N is carrier lifetime, τ_p is photon lifetime, α is linewidth enhancement factor, J is bias current, κ_f and τ_f are feedback rate and delay, respectively. (See the laser parameters in Ref. 18.) The light $E(t) = A(t)\exp(i2\pi\nu_0 t)$ from the laser with optical feedback will pass the filter and circulate in the ring, and thus the FRR's output is the result of multiple delayed-beam interference. Considering the superposition of the circulating field in fiber ring[26] and the filter response, the output field equation of the FRR can be expressed as

$$E_o(t) = i\sqrt{k}\left[E(t) - \frac{1-k}{k}\sum_{n=1}(i\sqrt{g})^n E(t-nT) * \underbrace{h(t)\cdots h(t)}_{n}\right]. \quad (3)$$

Here, k is coupling coefficient, T and g are ring's round-trip time and gain which is below 1 owing to external injection, h is filter response function, n is circulation times, and the asterisk means convolution. In simulations, we set $k = 0.2$ and assume the filter as a Lorentzian one with linewidth $\Lambda = 20$ GHz, i.e., the Fourier transform of h is $[1 + 2i(\nu - \nu_F)/\Lambda]^{-1}$.

We can numerically reproduce experimental observations under the model. By solving the rate equations with $\kappa_f = 10.84\ \text{ns}^{-1}$, $\tau_f = 5$ ns, and J of 1.76 times threshold, we obtained a laser chaos that has typical PSD (see Fig. S2(b) in supplementary material[29]) like the black (blue) curve in Fig. 2. According to Eq. (3), the interference will convert the laser phase into intensity nonlinearly through cosine function. Therefore, in Fig. 5(a), we first demonstrate the spectral property of $\cos\varphi$ that cannot be measured experimentally. Clearly, it presents a flat profile spreading over 10 GHz without prominent peaks, which is different from that of laser intensity chaos. Under $\Delta\nu = 20$ GHz and $g = 0.999$, Eq. (3) gives a PSD plotted by the black curve in Fig. 5(b), which

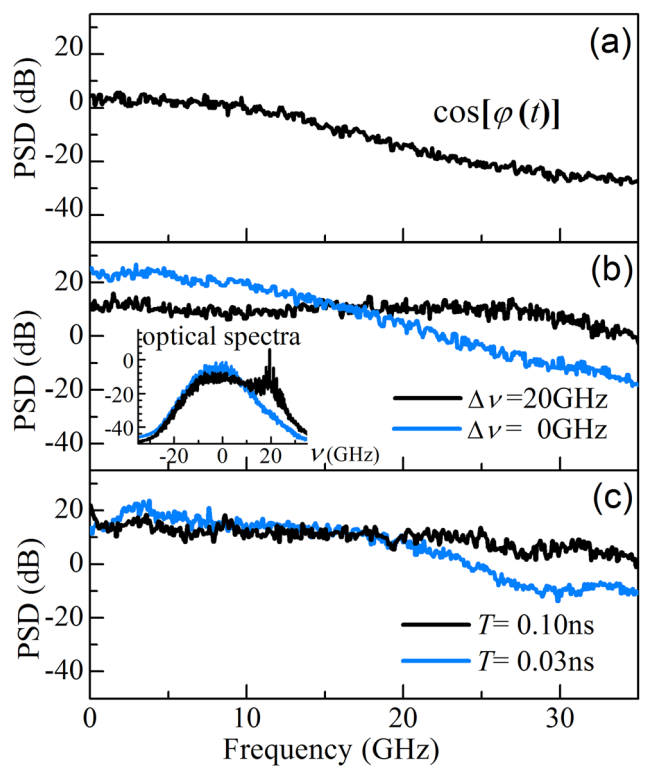

FIG. 5. Numerical PSD: (a) $\cos\varphi$ of chaotic laser; (b) outputs at $\Delta\nu = 20$ (black) and $\Delta\nu = 0$ GHz (gray, azure), $T = 5$ ns, and the inset plots the corresponding optical spectra; (c) outputs at $T = 0.1$ (black) and $T = 0.03$ ns (gray, azure), $\Delta\nu = 20$ GHz.

reveals that the broadband chaos can reach beyond 30 GHz. As $\Delta v = 0$ GHz and $g = 0.6$, the spectrum turns into the profile shown as the gray (azure) curve. The corresponding optical spectra are displayed in the inset. These numerical results agree well with the experimental results plotted in curves (4) and (3) in Fig. 4(a). The simulation predicts that the power spectrum can be further enhanced by making laser phase dynamics faster, for instance, through increasing feedback strength.

Note that the optical spectrum at large filter detuning mainly contains two components: the remaining laser mode and the gained filter mode. Therefore, we attribute the expansion of power spectrum through the ring resonator to the fact that the multiple-beam interference converts laser phase into intensity by two kinds of beating. One is the beating between the remaining laser mode and gained filter mode, resulting in high-frequency wideband oscillations; the other is the delayed self-beating in the remaining laser mode, which enhances the low-frequency oscillations below the laser relaxation frequency. The combination of these two beatings broadens and smoothes the chaotic spectrum. It should be mentioned that zero detuning only causes the delayed self-beating, and shown in azure line in Fig. 5(b) the corresponding output PSD is similar to that of $\cos\varphi$. This means that the delayed self-beating improves spectral profile as low-pass type. Because the self-beating always exists, the spectral profile and flatness remain during the control of bandwidth by filter adjustment, as experimentally observed.

Under the model, we further studied the influences of ring's round-trip time T with filter detuning of 20 GHz. As shown in Fig. 5(c), when round-trip time reduces to 0.1 ns, the spectrum (black) is still wideband, which is similar to that of $T = 5$ ns. As T decreases to 0.03 ns, that is the coherence time of chaotic laser (see Fig. S2(d) in supplementary material[29]), the spectrum becomes narrower, as displayed by the gray (azure) line. This is caused by the coherence of the two adjacent delayed beams $E(t - nT)$ and $E(t - (n + 1)T)$. Despite this, the spectrum still flatly extends over 20 GHz. The fiber ring resonator, therefore, can be shortened to a small size of several centimeters for applications of integration.

As we mentioned above, the physical process in the proposed method takes place in the fiber ring resonator rather than in the laser cavity, which is different from the previous technique that injects light into chaotic laser or vice versa.[14–20] The difference brings about two significant advantages over the previous. First, owing to the introduction of self-beating instead of laser dynamics, the resonator flattens the whole spectrum and removes the feature of relaxation oscillation. The spectral flatness of ± 1.5 dB is close to that of spontaneous emission noise,[32] which means uniform energy distribution. In contrast, the previous method cannot hide the relaxation peak and flatten the whole spectrum because the laser dynamics is involved.[18] Even though dual injection can enlarge bandwidth to 38 GHz,[19] the whole spectrum is still band-pass profile contained with a range of about ± 7.1 dB. Second, according to the numerical model, the resonator method can get broadband spectrum and similar control law so long as the input light is chaotic with fast phase variation. In other words, the resonator is suitable for different chaotic light sources, such as laser subject to optical feedback, optical injection, or optoelectronic feedback. On the contrary, the previous method is governed by the chaotic laser rate equations with added injection term,[18] and thus is susceptible to the state or structure of the chaotic laser. For instance, the behavior of optical-feedback laser with added injection[18] is different from the case of an optical-injected laser.[33]

To sum up, the fiber ring resonator equipped with an optical filter and an amplifier actually is a bandwidth enhancer that can widen and flatten the power spectral density of chaotic semiconductor laser. Both experiments and simulations show that the method is of practical merits, because of its simple and integratable setup and potential for controlling the spectrum profile to meet different application needs. For example, large filter detuning produces ultra-wide bandwidth for fast random number generation, while small detuning brings high-energy signal for lidar or reflectometry.

This work was supported by the National Natural Science Foundation of China (NSFC) (Grant Nos. 60908014, 60927007, 61108027, and 612278121), the Natural Science Foundation for Young Scientists (2009021003), and by the Key Science and Technology Program (20100321055-02) of Shanxi Province, China.

[1]A. Argyris, D. Syvridis, L. Larger, V. Annovazzi-Lodi, P. Colet, I. Fischer, J. García-Ojalvo, C. R. Mirasso, L. Pesquera, and K. A. Shore, Nature **438**, 343 (2005).
[2]R. Lavrov, M. Jacquot, and L. Larger, IEEE J. Quantum Electron. **46**, 1430 (2010).
[3]A. Uchida, K. Amano, M. Inoue, K. Hirano, S. Naito, H. Someya, I. Oowada, T. Kurashige, M. Shiki, S. Yoshimori, K. Yoshimura, and P. Davis, Nat. Photon. **2**, 728 (2008).
[4]I. Reidler, Y. Aviad, M. Rosenbluh, and I. Kanter, Phys. Rev. Lett. **103**, 024102 (2009).
[5]F. Y. Lin and J. M. Liu, IEEE J. Sel. Top. Quantum Electron. **10**, 991 (2004).
[6]Y. C. Wang, B. J. Wang, and A. B. Wang, IEEE Photon. Technol. Lett. **20**, 1636 (2008).
[7]A. B. Wang, M. J. Zhang, H. Xu, and Y. C. Wang, IEEE Electron Device Lett. **32**, 372 (2011).
[8]Y. Takeuchi, R. Shogenji, and J. Ohtsubo, Appl. Phys. Lett. **93**, 181105 (2008).
[9]A. Argyris, M. Hamacher, K. E. Chlouverakis, A. Bogris, and D. Syvridis, Phys. Rev. Lett. **100**, 194101 (2008).
[10]A. Argyris, E. Grivas, M. Hamacher, A. Bogris, and D. Syvridis, Opt. Express **18**, 5188 (2010).
[11]V. Z. Tronciu, C. Mirasso, P. Colet, M. Hamacher, M. Benedetti, V. Vercesi, and V. Annovazzi-Lodi, IEEE J. Quantum Electron. **46**, 1840 (2010).
[12]S. Sunada, T. Harayama, K. Arai, K. Yoshimura, P. Davis, K. Tsuzuki, and A. Uchida, Opt. Express **19**, 5713 (2011).
[13]K. Hirano, K. Amano, A. Uchida, S. Naito, M. Inoue, S. Yoshimori, K. Yoshimura, and P. Davis, IEEE J. Quantum Electron. **45**, 1367 (2009).
[14]A. Uchida, T. Heil, Y. Liu, P. Davis, and T. Aida, IEEE J. Quantum Electron. **39**, 1462 (2003).
[15]K. Hirano, T. Yamazaki, S. Morikatsu, H. Okumura, H. Aida, A. Uchida, S. Yoshimori, K. Yoshimura, T. Harayama, and P. Davis, Opt. Express **18**, 5512 (2010).
[16]Y. Takiguchi, K. Ohyagi, and J. Ohtsubo, Opt. Lett. **28**, 319 (2003).
[17]A. B. Wang, Y. C. Wang, and H. C. He, IEEE Photon. Technol. Lett. **20**, 1633 (2008).
[18]A. B. Wang, Y. C. Wang, and J. F. Wang, Opt. Lett. **34**, 1144 (2009).
[19]M. J. Zhang, T. G. Liu, P. Li, A. B. Wang, J. Z. Zhang, and Y. C. Wang, IEEE Photon. Technol. Lett. **23**, 1872 (2011).
[20]S. Y. Xiang, W. Pan, B. Luo, L. S. Yan, X. H. Zou, N. Li, and H. N. Zhu, IEEE J. Quantum Electron. **48**, 1069 (2012).

[21]R. Lavrov, M. Peil, M. Jacquot, L. Larger, V. Udaltsov, and J. Dudley, Phys. Rev. E **80**, 026207 (2009).
[22]K. E. Callan, L. Illing, Z. Gao, D. J. Gauthier, and E. Schöll, Phys. Rev. Lett. **104**, 113901 (2010).
[23]M. Nourine, Y. K. Chembo, and L. Larger, Opt. Lett. **36**, 2833 (2011).
[24]J. M. Choi, R. K. Lee, and A. Yariv, Opt. Lett. **26**, 1236 (2001).
[25]J. W. Dawson, N. Park, and K. J. Vahala, IEEE Photon. Technol. Lett. **4**, 1063 (1992).
[26]J. Capmany, B. Ortega, and D. Pastor, J. Lightwave Technol. **24**, 201 (2006).
[27]L. F. Stokes, M. Chodorow, and H. J. Shaw, Opt. Lett. **7**, 288 (1982).
[28]M. T. Rosenstein, J. J. Collins, and C. J. De Luca, Physica D **65**, 117 (1993).
[29]See supplementary material at http://dx.doi.org/10.1063/1.4789366 for an experimental result obtained when the input laser was in an undeveloped chaos state (Fig. S1), and for a numerical demonstration of the properties of chaotic laser with optical feedback (Fig. S2).
[30]A. Uchida, *Optical Communication with Chaotic Lasers* (Wiley-VCH Verlag & Co. KGaA, Weinheim, 2012), p. 45.
[31]R. Long and K. Kobayashi, IEEE J. Quantum Electron. **16**, 347 (1980).
[32]X. Li, A. B. Cohen, T. E. Murphy, and R. Roy, Opt. Lett. **36**, 1020 (2011).
[33]N. M. Al-Hosiny, I. D. Henning, and M. J. Adams, Opt. Commun. **269**, 166 (2007).